The EMBO Journal (2011) 30, 3647–3661 | © 2011 European Molecular Biology Organization | Some Rights Reserved 0261-4189/11
www.embojournal.org

THE EMBO JOURNAL

EMBO open

Vaccinia extracellular virions enter cells by macropinocytosis and acid-activated membrane rupture

Florian Ingo Schmidt[1], Christopher Karl Ernst Bleck[2], Ari Helenius[1] and Jason Mercer[1,*]

[1]Institute of Biochemistry, ETH Zurich, Zurich, Switzerland and [2]Center for Cellular Imaging and Nano Analytics (C-CINA), Biozentrum, University of Basel, Basel, Switzerland

Vaccinia virus (VACV), the model poxvirus, produces two types of infectious particles: mature virions (MVs) and extracellular virions (EVs). EV particles possess two membranes and therefore require an unusual cellular entry mechanism. By a combination of fluorescence and electron microscopy as well as flow cytometry, we investigated the cellular processes that EVs required to infect HeLa cells. We found that EV particles were endocytosed, and that internalization and infection depended on actin rearrangements, activity of Na^+/H^+ exchangers, and signalling events typical for the macropinocytic mechanism of endocytosis. To promote their internalization, EVs were capable of actively triggering macropinocytosis. EV infection also required vacuolar acidification, and acid exposure in endocytic vacuoles was needed to disrupt the outer EV membrane. Once exposed, the underlying MV-like particle presumably fused its single membrane with the limiting vacuolar membrane. Release of the viral core into the host cell cytosol allowed for productive infection.

The EMBO Journal (2011) **30,** 3647–3661. doi:10.1038/emboj.2011.245; Published online 26 July 2011
Subject Categories: membranes & transport; microbiology & pathogens
Keywords: acid-activated rupture; extracellular virion; macropinocytosis; poxvirus; vaccinia virus

Introduction

To successfully replicate, viruses have to deliver their genome and accessory proteins into the cytosol or nucleus of a host cell. This implies that virus particles or their packaged genome must cross the plasma membrane (PM) or the limiting membrane of endocytic vacuoles. In the case of animal viruses that have a lipid bilayer envelope, the critical step of membrane penetration involves fusion of the viral membrane with a cellular membrane. The packaged genome is thus released into the cytosol (Marsh and Helenius, 2006).

*Corresponding author. Institute of Biochemistry, ETH Zurich, ETH Hoenggerberg—HPM E9.1, Schafmattstr. 18, Zurich 8093, Switzerland. Tel.: +41 44 632 5818; Fax: +41 44 632 1269;
E-mail: jason.mercer@bc.biol.ethz.ch

Received: 17 January 2011; accepted: 29 June 2011; published online: 26 July 2011

Vaccinia virus (VACV) is the prototypic poxvirus and is closely related to variola virus, the causative agent of smallpox (Damon 2007). Poxviruses are enveloped DNA viruses that use a fusion mechanism to enter cells (Senkevich *et al*, 2005). They are unusual because they exist in two different, infectious forms (Moss 2007). In addition to single membrane containing particles (mature virions, MVs) (Hollinshead *et al*, 1999; Cyrklaff *et al*, 2005), particles are produced that contain two concentric membranes (extracellular virions, EVs) (Smith *et al*, 2002). MVs are released after lysis of infected cells and mediate host-to-host transmission (Smith *et al*, 2003; Moss 2007). EVs leave the cell by exocytosis and are required for virus spread within a tissue or from tissue to tissue (Payne, 1980). An EV particle consists of an MV-like particle surrounded by an additional membrane containing cellular proteins and at least six viral proteins unique to the EV (Payne, 1978, 1979; Smith *et al*, 2002). With two membranes, a conventional mechanism of entry is not possible. Loss of the outer membrane by fusion would release a particle into the cytosol that is still covered by the inner membrane. Such a particle is unlikely to cause productive infection.

Recent studies have shown that the majority of MVs enter cells by endocytosis and penetration occurs by membrane fusion in intracellular vacuoles (Townsley *et al*, 2006; Townsley and Moss, 2007). The entry process involves macropinocytic internalization induced by phosphatidylserine (PS) exposed on the MV membrane (Zwartouw, 1964; Ichihashi and Oie, 1983; Huang *et al*, 2008; Mercer and Helenius, 2008; Mercer *et al*, 2010).

Available information on EV entry suggests that the outer of the two membranes is simply lost or ruptured revealing the underlying MV-like membrane, which then undergoes fusion with the PM or the limiting membrane of a vacuole (Moss, 2006). The core could thus be delivered into the cytosol without a membrane. The model proposing rupture of the outer membrane of the EV is based on the following observations: (1) The entry/fusion complex (EFC) present in the inner of the two membranes is essential for EV infection (Senkevich *et al*, 2004a, b). (2) The outer membrane of the EV is fragile and sensitive to *in vitro* treatment with reduced pH and anionic polysaccharides (Ichihashi, 1996; Vanderplasschen *et al*, 1998a; Law *et al*, 2006). EV disruption with anionic polysaccharides has been shown to depend on two EV-specific proteins, A34 and B5 (Law *et al*, 2006; Roberts *et al*, 2009). (3) Electron micrographs of cell surface bound EVs show the presence of ruptured EV membranes covering MV-like particles (Law *et al*, 2006).

However, it has been observed that antibodies directed against MV-membrane proteins that neutralize MV infection, fail to neutralize infection by EVs (Ichihashi, 1996; Vanderplasschen *et al*, 1998a). This suggests that upon rupture of the outer EV membrane, the underlying MV-like

particle is inaccessible to antibodies. One explanation could be that EV rupture takes place at the PM and the disrupted outer membrane covers the PM-bound MV-like particle. Another possibility is that rupture occurs only after endocytic internalization of the intact EV particle. Several studies have addressed the EV entry process using epithelial cell lines and human monocyte-derived dendritic cells (DCs) with conflicting results (Ichihashi, 1996; Vanderplasschen *et al*, 1998a; Locker *et al*, 2000; Law *et al*, 2006; Roberts *et al*, 2009; Sandgren *et al*, 2010).

In this study, we used flow cytometry-based assays and microscopy in combination with different perturbants of cellular proteins and functions to analyse EV infection of HeLa cells. We found that VACV EVs induced their own endocytic uptake by macropinocytosis. Acidification of endocytic compartments was needed to trigger disruption of EV membranes, presumably followed by fusion of the underlying virus particles with limiting membranes of endocytic organelles. This would release virus cores into the cytosol and allow productive infection.

Results

Quality of EV particles

In our study, we used EVs released into the medium as free particles by infected cells. They correspond to the population of VACV particles responsible for long-range spread in the infected organism (Payne, 1980). The outer membrane of EVs is fragile and easily disrupted during purification (Ichihashi, 1996; Vanderplasschen and Smith, 1997) (our unpublished results). We therefore used freshly produced EVs of VACV strains Western Reserve (WR) and International Health Department J (IHD-J) in clarified supernatants of infected RK13 cells without further purification.

To quantify the fraction of intact EVs, we used the monoclonal antibody (MAb) 7D11, which binds to the L1 protein in the MV membrane, and selectively neutralizes MVs and broken EVs (Figure 1A) (Wolffe *et al*, 1995). Using plaque assays, we determined that MVs of VACV strains WR and IHD-J were neutralized by 5 μg/ml 7D11. Depending on the preparation, 10–40% of WR and IHD-J infectivity in the supernatant was insensitive to 7D11 and therefore represented infectivity caused by intact EVs. In contrast, WR ΔA34R, a deletion mutant of the EV membrane protein A34 known to contain stabilized EV membranes (Law *et al*, 2006; Husain *et al*, 2007), was ~90% insensitive to 7D11.

To confirm the presence of intact EVs in the supernatant, we analysed VACV particles released from RK13 cells by confocal microscopy. To discriminate between MVs and EVs, we used a recombinant IHD-J strain expressing two different fluorescent fusion proteins: mCherry was fused to the core protein A5 and GFP to the EV-specific outer membrane protein F13. Both MVs and EVs therefore contained a red fluorescent core and could be visualized as discrete spots. The majority of particles in the supernatant of infected RK13 cells (83%) was also positive for the outer EV membrane (green fluorescent). Some green fluorescent particles without a red fluorescent core were observed, likely representing EV

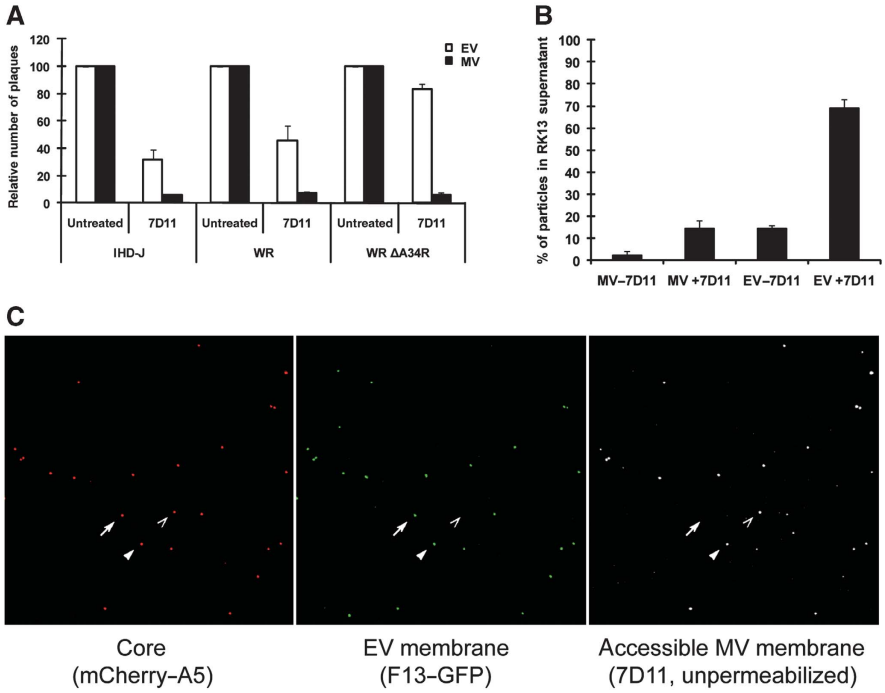

Figure 1 Quality of EV particles. (**A**) EV quality—infectious particles. Clarified supernatants of RK13 cells infected with VACV IHD-J, WR, or WR ΔA34R were titrated on BSC-40 cells after incubation with or without Mab 7D11. As a control, purified MVs of the same strains were subjected to the same treatment and titration. Plaque numbers were normalized to untreated virus samples. Results represent the average of three independent experiments (mean ± s.e.m.). (**B**) EV quality—fluorescent particles. Clarified supernatants of RK13 cells infected with IHD-J mCherry–A5 F13–GFP were incubated with 7D11, bound to cover slips, and fixed. 7D11 was visualized with AF 647 goat anti-mouse and images recorded by confocal microscopy. Virus particles were detected by their fluorescent core and assigned to the following categories: MV−7D11 (mCherry), MV + 7D11 (mCherry and 7D11 staining), EV−7D11 (mCherry, GFP), or EV + 7D11 (mCherry, GFP, and 7D11 staining). Average values of three independent experiments are shown ± s.e.m. (**C**) Fluorescent EVs. Representative images from (**B**). Examples of a neutralized MV (MV + 7D11, open arrowhead), an intact EV (EV−7D11, arrow), and a disrupted EV (EV + 7D11, closed arrowhead) are highlighted.

membranes that had lost the core (15 spots per 100 virus cores, data not shown).

To determine the fraction of intact EVs, cell supernatants containing recombinant IHD-J viruses were preincubated with 7D11, applied to a cover slip, and stained with a fluorescently labelled secondary antibody. MVs and broken EVs with exposed L1 were expected to be stained whereas intact EVs were not. Figure 1C shows a field with MVs (mCherry and 7D11 staining; open arrowhead), disrupted EVs (mCherry, GFP, and 7D11 staining; closed arrowhead), and intact EVs (mCherry and GFP, arrow). Analysis of >600 virus particles in three independent experiments showed that 17% of the viruses were MVs, 69% were disrupted EVs, and 14% were intact EVs (Figure 1B). This amount of intact EVs corresponded to the fraction of 7D11-insensitive EVs determined by plaque assay for the same supernatants (data not shown).

After analysing EV particles for both infectivity and integrity, we concluded that MAb 7D11 could be used to discriminate between intact and broken EVs. It was evident that the majority of IHD-J and WR EVs released into the supernatant did not possess an intact second membrane. In most instances—judging by the presence of F13–GFP—the disrupted EV membrane remained associated with the virus particle. Disruption of the outer membrane did not interfere with the infectivity of EVs.

EV particles are endocytosed

For productive infection, both EV membranes must be removed during the entry process. While it has been suggested that removal of the outer membrane of EVs happens already on the PM (Law *et al*, 2006), it is conceivable that the EV particles are endocytosed first with loss of the outer EV membrane taking place in endocytic compartments.

To test whether EVs can be internalized with their outer membrane still in place, we used recombinant IHD-J EVs containing F13–GFP to infect HeLa cells for 30 min at 37°C. Samples were stained for the EV membrane protein B5 under non-permeabilizing conditions to distinguish between external and intracellular EVs (Figure 2B). A fraction of EV particles (green spots; white arrows, inset) was inaccessible to antibody staining, indicating they were internalized. To control for changes in the B5 epitope or inappropriate staining, the same procedure was performed either with cells in which the virus had not been allowed to internalize (bound EVs, Figure 2A) or with cells permeabilized with saponin after fixation (Figure 2C). In both conditions, all EV particles were stained for B5.

To assure that intact EV particles, and not only dissociated EV membranes without cores were internalized, HeLa cells were infected with IHD-J mCherry–A5 F13–GFP EVs and subjected to B5 staining under non-permeabilizing conditions (Figure 2D). That a subpopulation of the dual-coloured EVs was not stained (white arrows, inset) indicated that EV particles were internalized with the outer membrane. Virus cores or MVs without an EV membrane (closed arrowhead) and internalized EV membranes without a core (open arrowhead) were also observed. These may represent intermediates of the EV entry process or may have been internalized from the inocculum.

To confirm these findings, HeLa cells incubated with IHD-J F13–GFP EVs for 30 min were analysed by electron microscopy for the presence of internalized particles with EV membranes. Ultrathin sections of cells were subjected to negative staining to visualize the EV membrane. Immunogold labelling directed against GFP was used to detect the F13–GFP fusion protein in the EV membrane (Figure 2E and F; Supplementary Figure S1). Gold-labelled EV particles were found both at the PM, often next to membrane protrusions (Figure 2E; Supplementary Figure S1A and B), and in intracellular vesicles (Figure 2E and F; Supplementary Figure S1A–F). In some particles, two membranes could be clearly distinguished (arrows in Figure 2F; Supplementary Figure S1D), confirming that full EV particles were endocytosed. In a few particles (Supplementary Figure S1F), the EV membrane was partly disrupted. EV membranes devoid of cores were also observed bound to the PM. They may have originated from free membranes in the inoculum, or from particles disrupted at the PM.

Internalization of EVs was confirmed using flow cytometry. IHD-J F13–GFP EVs were bound to HeLa cells on ice and incubated either on ice or at 37°C for a further 30 min. Bound virus particles were removed by trypsin digestion and the cells were subjected to flow cytometry to determine the cell-associated fluorescence from internalized particles (Figure 3A and B). The low temperature control showed that bound EVs could be almost completely removed by trypsin, whereas cells incubated at 37°C were green fluorescent, confirming the presence of internalized IHD-J F13–GFP EVs. When cells were detached with EDTA, fluorescence of both bound and internalized EVs could be measured (Figure 3A and C). Fluorescence intensities with and without incubation at 37°C were comparable, confirming that GFP fluorescence and virus binding was not affected by incubation at 37°C.

These experiments showed that cell-bound EVs were rapidly internalized by endocytosis. Although disrupted EVs were not distinguished from intact EVs in these experiments, we could show by fluorescence microscopy, electron microscopy, and flow cytometry that the outer membrane of EVs was not lost before internalization.

EVs are internalized by macropinocytosis

To analyse the endocytic mechanism responsible for EV internalization, and to test whether endocytosis was required for infection by intact EVs, we infected HeLa cells in the presence of a spectrum of small compound inhibitors known to affect endocytic processes. GFP-expressing viruses and flow cytometry were used to quantify infection by VACV EVs of the strains IHD-J and WR (Figure 4A and C).

To assure that infection by intact EVs was specifically analysed, we pretreated EV-containing supernatants with Mab 7D11 for all infection experiments. Since cells infected with VACV WR released less EVs into the medium than cells infected with strain IHD-J, WR EV supernatants were concentrated by sedimentation before MV neutralization. This did not significantly reduce the fraction of intact EVs (data not shown). In all cases, MVs were used as controls. IHD-J and WR MVs have been found to induce macropinocytosis in host cells, and to use this pathway as a route of productive infection (Mercer and Helenius, 2008).

Inhibition of clathrin-mediated endocytosis by chlorpromazine (Chlo) affected neither IHD-J EV nor MV infection (Figure 4A). Infection with EVs and MVs was only moderately affected by the general protein kinase inhibitor

staurosporine (Stau), and it was not influenced by the tyrosine-kinase inhibitor genistein (Geni) or the posphoinositide 3-kinase inhibitor wortmannin (Wort). In contrast, infection with both EVs and MVs was dramatically blocked by Iressa, an inhibitor of the epidermal growth factor receptor (EGFR); by the protein kinase C (PKC) inhibitor calphostin C

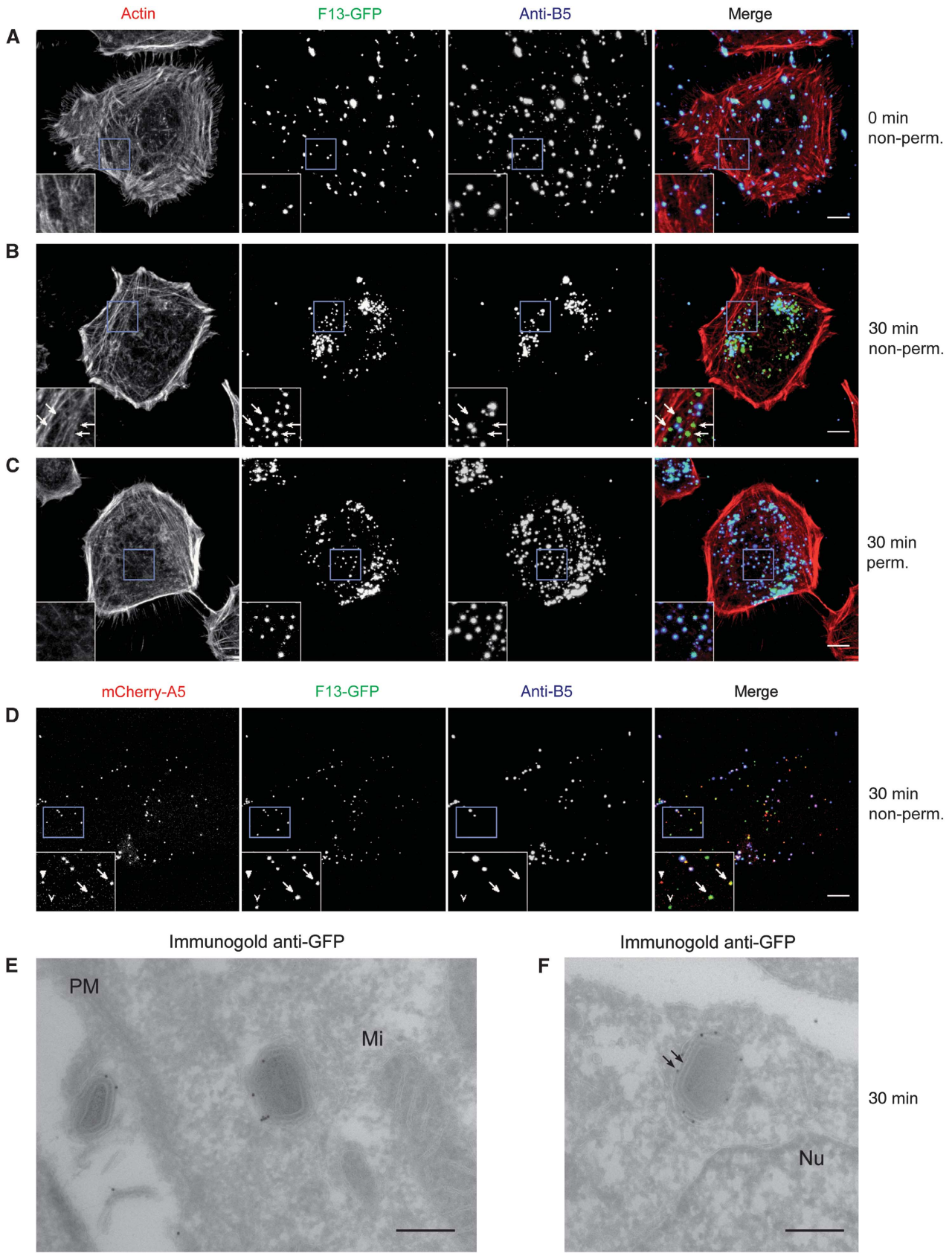

(CalC); by 3-indolepropionic acid (IPA-3), an inhibitor of p21-activated kinase 1 (PAK1); and by the smooth muscle myosin light chain kinase (smMLCK) inhibitor ML-7. Rottlerin (Rott), originally described to specifically inhibit PKCδ (Gschwendt *et al*, 1994), but later found to have multiple effects (Davies *et al*, 2000; Soltoff, 2001; Kayali *et al*, 2002; Tillman *et al*, 2003), nearly abolished infection. Perturbation of actin dynamics with cytochalasin D (Cyto) and jasplakinolide (Jasp) strongly reduced EV infection; the block of infection was, however, even more pronounced for MVs. An inhibitor of Na^+/H^+ antiporters, ethylisopropyl amiloride (EIPA), also efficiently prevented infection with both EVs and MVs. The requirement of PAK1, smMLCK, PKC activity, actin dynamics, and sodium–proton exchangers strongly suggested an endocytic process categorized as macropinocytosis (Mercer and Helenius, 2009).

To determine if the inhibitors of infection blocked macropinocytic uptake of EVs, we quantified internalization of IHD-J EVs and MVs using flow cytometry (Figure 4B). For EV internalization experiments, IHD-J EVs containing F13–GFP were used without neutralization as 7D11 treatment did not affect endocytic uptake of neutralized, disrupted EVs (data not shown). For MV internalization experiments, MV particles incorporating EGFP–A5 in the core were employed (Supplementary Figure S2). Bound MVs, in contrast to EVs, were only partially removed by trypsin digestion (sample MV 0°C (int.)). Signal intensity of cells incubated at 37°C was significantly higher than that of cells kept at 0°C allowing for quantification after background subtraction. Rott, IPA-3, Cyto, Jasp, and EIPA efficiently blocked internalization of both EVs and MVs, confirming that the observed effects on infection occurred due to impaired endocytic uptake.

The inhibitors that blocked IHD-J EV infection were then tested against WR EVs (Figure 4C). Inhibition of EGFR, PAK1, smMLCK, PKC, actin dynamics, and Na^+/H^+ antiport caused a strong reduction of WR EV infection. These results indicated that EVs of both IHD-J and WR strains exploited macropinocytosis for infection.

Throughout these infection experiments, neutralized MVs and neutralized disrupted EVs were present in the inocula. Thus, it was conceivable that these particles—although neutralized by antibody binding—stimulated macropinocytosis, resulting in the co-internalization of intact EVs. To test whether MVs stimulated the internalization of EVs, we performed infection assays with a GFP-expressing version of the mutant virus WR ΔA34R, a virus that produces ~90% intact EVs (Figure 4D). EV infection was reduced by the same

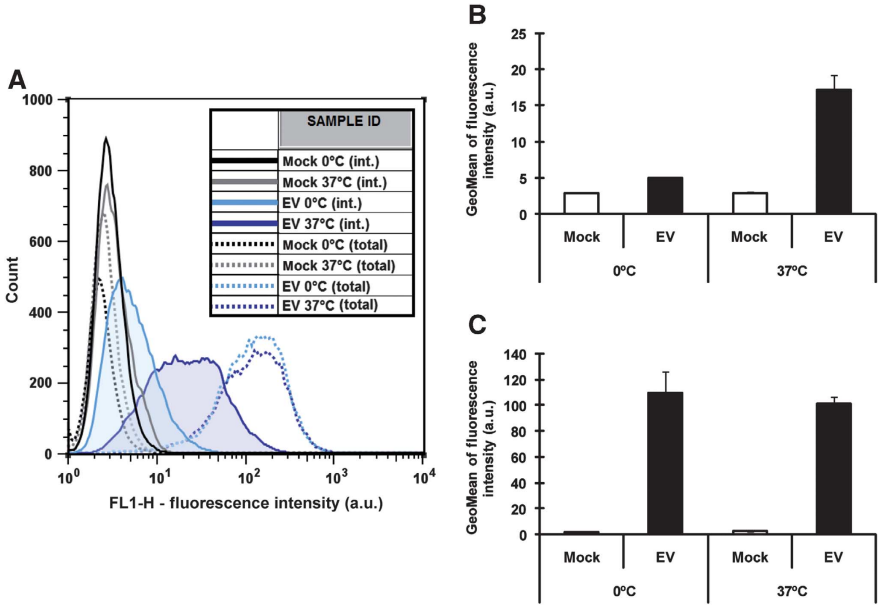

Figure 3 EV internalization by flow cytometry. IHD-J F13–GFP EVs (MOI 175) were bound to HeLa cells on ice for 1 h and cells incubated at 0 or 37°C for 30 min. To detect internalized EVs (int.), bound virions were removed and cells were detached with trypsin; to measure total cell-associated virions (total), cells were detached with EDTA. Cells were fixed, and green fluorescence quantified by flow cytometry. Representative histograms of untreated samples are shown in (**A**); green fluorescence intensity from three independent experiments was quantified and the average of measured geometric means of internalized (**B**) and total (**C**) EVs is displayed ± s.e.m.

Figure 2 EV internalization by fluorescence and electron microscopy. (**A**–**D**) IHD-J F13–GFP EVs (**A**–**C**) or IHD-J mCherry–A5 F13–GFP EVs (**D**) were bound to HeLa cells on ice for 1 h (MOI 15). EV particles were stained with VMC-20 (anti-B5) directly (**A**) or after incubation at 37°C for 30 min (**B**–**D**). VMC-20 staining was performed either under non-permeabilizing (non-perm.) conditions to visualize bound virions (**A**, **B**, **D**) or under permeabilizing (perm.) conditions to visualize bound and internalized virions (**C**). Images were recorded by confocal microscopy and representative maximum projections of *Z*-stacks are shown. Arrows in the inset of B highlight F13–GFP-containing EV membranes not accessible to VMC-20 staining. In the inset of (**D**), EV particles (arrows) and an EV membrane without a core (open arrowhead), all not accessible to VMC-20 staining, as well as a virus core or MV without an EV membrane (closed arrowhead), are highlighted. Scale bars = 10 μm. (**E**, **F**) IHD-J F13–GFP EVs were bound to HeLa cells on ice for 1 h (MOI 300). Cells were incubated at 37°C for 30 min, fixed, and subjected to cryosectioning and immunolabelling with anti-GFP and protein A-gold. Images were recorded by transmission electron microscopy and representative pictures are shown. Arrows in (**F**) highlight MV and EV membranes. Mi, mitochondrion; Nu, nucleus. Scale bars = 200 nm.

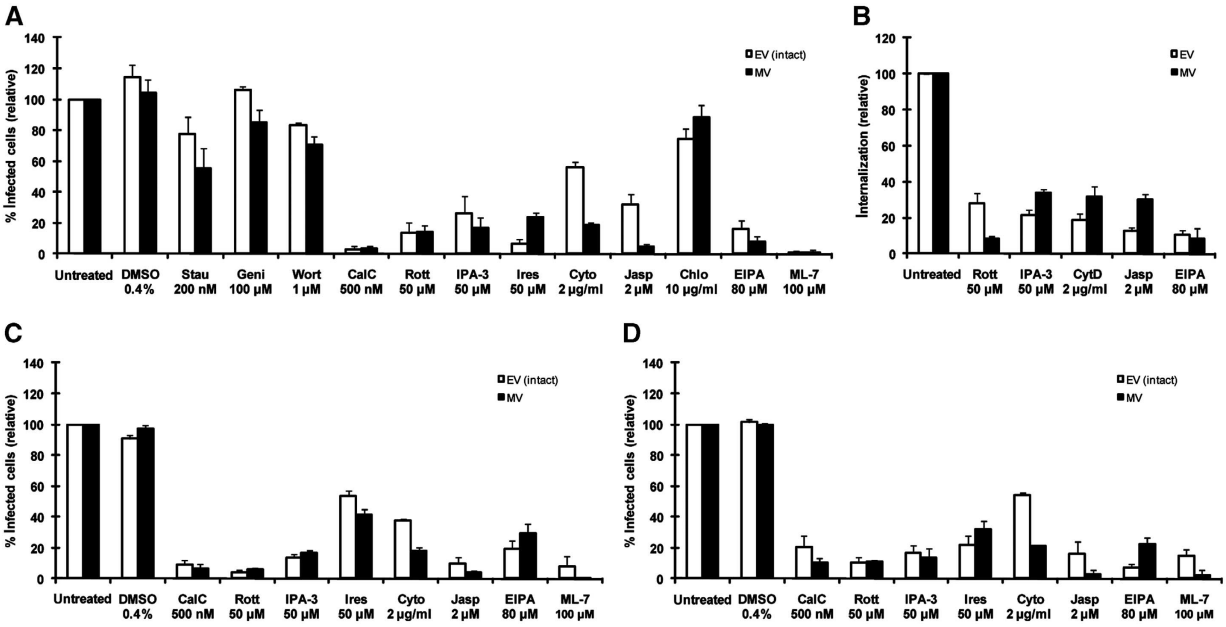

Figure 4 Cellular factors required for EV infection. (**A**–**D**) HeLa cells were left untreated or treated with DMSO (highest used concentration), staurosporine (Stau), genistein (Geni), wortmannin (Wort), calphostin C (CalC), rottlerin (Rott), 3-indolepropionic acid (IPA-3), Iressa (Ires), chlorpromazine (Chlo), ML-7 (all 30 min), cytochalasin D (Cyto), jasplakinolide (Jasp), or ethylisopropyl amiloride (EIPA) (all 15 min). MVs or EVs of IHD-J GFP (**A**), WR GFP (**C**), or WR ΔA34R GFP (**D**) were preincubated in the presence of drugs and in the case of EVs with 7D11 (MOI 2). Cells were infected and green fluorescent cells quantified 4 h p.i. by flow cytometry. Infection levels were normalized to untreated samples. (**B**) EV (IHD-J F13–GFP) and MV (IHD-J EGFP–A5) internalization in the presence of various drugs was quantified as described in Figure 3. The geometric mean of green fluorescence intensity of 0°C samples was substracted from 37°C samples and internalization normalized to untreated samples. All experiments were performed three times independently, mean values ± s.e.m. are shown.

panel of drugs as infection by EVs of wild-type IHD-J and WR. It was sensitive to Iressa, CalC, Rott, ML-7, IPA-3, actin perturbants, and EIPA, indicating that EV uptake by macropinocytosis was not influenced by the presence of neutralized, disrupted EVs or neutralized MVs. Along the same lines, we tested if the addition of excess amounts of neutralized MVs would boost infection by WR ΔA34R EVs (Supplementary Figure S3). Even when a 25-fold excess of neutralized MVs was used, no boost in EV infection was observed. These results indicated that VACV EVs of IHD-J and WR strains are capable of triggering macropinocytosis, resulting in internalization and productive infection of host cells.

EV particles induce macropinocytosis

Macropinocytosis can be distinguished from other types of endocytosis by a dramatic rearrangement of the actin cytoskeleton and by enhanced cellular fluid-phase uptake (Mercer and Helenius, 2009). To investigate cellular phenotypes of macropinocytosis, WR ΔA34R was used. The integrity of the EV membrane on WR ΔA34R EV particles allowed us to distinguish between EV- and MV-induced changes. If EVs use macropinocytosis for their internalization, increased uptake of fluid-phase markers would be expected. To test this, uptake of 10 kDa dextran-Alexa fluor (AF) 488 into serum-starved HeLa cells after stimulation with EVs and MVs was quantified by flow cytometry (Figure 5A). Indeed, uptake of dextran during a 10-min pulse was increased by 42 and 51%, respectively. In addition, we observed IHD-J F13–GFP EVs co-localizing with 10 kDa dextran-AF 594 in large intracellular vesicles (Supplementary Figure S4), suggesting that EV particles are internalized into macropinosomes.

Uptake of fluid by macropinocytosis requires the formation of dynamic membrane protrusions. These protrusions occur as lamellipodia, circular ruffles, or blebs. Functionally, they all lead to the formation of macropinosomes of irregular size and shape (Mercer and Helenius, 2009).

To determine if EVs induce the formation of membrane protrusions, HeLa cells were treated with EVs of WR ΔA34R EGFP–A5. MVs known to induce blebbing (Mercer and Helenius, 2008) were used as a control. Virus particles were bound to HeLa cells and incubated at 37°C for 40 min. Cells were fixed and analysed by differential interference contrast (DIC) and wide-field fluorescence microscopy (Figure 5B and C). A low level of membrane blebbing was observed in mock-treated cells (3%), whereas 20–70% of all cells treated with different amounts of EVs or MVs exhibited extensive, systemic bleb formation.

The finding that WR ΔA34R EVs triggered both fluid-phase uptake and extensive blebbing confirmed the capacity of EVs to induce macropinocytosis at a level similar to that seen for MVs.

Uptake of MVs by macropinocytosis has been shown to be triggered by PS, a phospholipid enriched in the MV membrane. When PS in the MV membrane is masked by the PS-binding protein annexin V (ANX5), MV infection is almost completely blocked (Mercer and Helenius, 2008). If EVs induce macropinocytosis through a similar mechanism, EV infection would be expected to be blocked by ANX5 as well. To test this, EVs and MVs of WR ΔA34R GFP were pretreated with ANX5 and used for infection experiments (Figure 5D). While MV infectivity was reduced to 38% by ANX5, EV infection was not affected. This suggested that VACV EVs induce macropinocytosis through a different trigger than MVs.

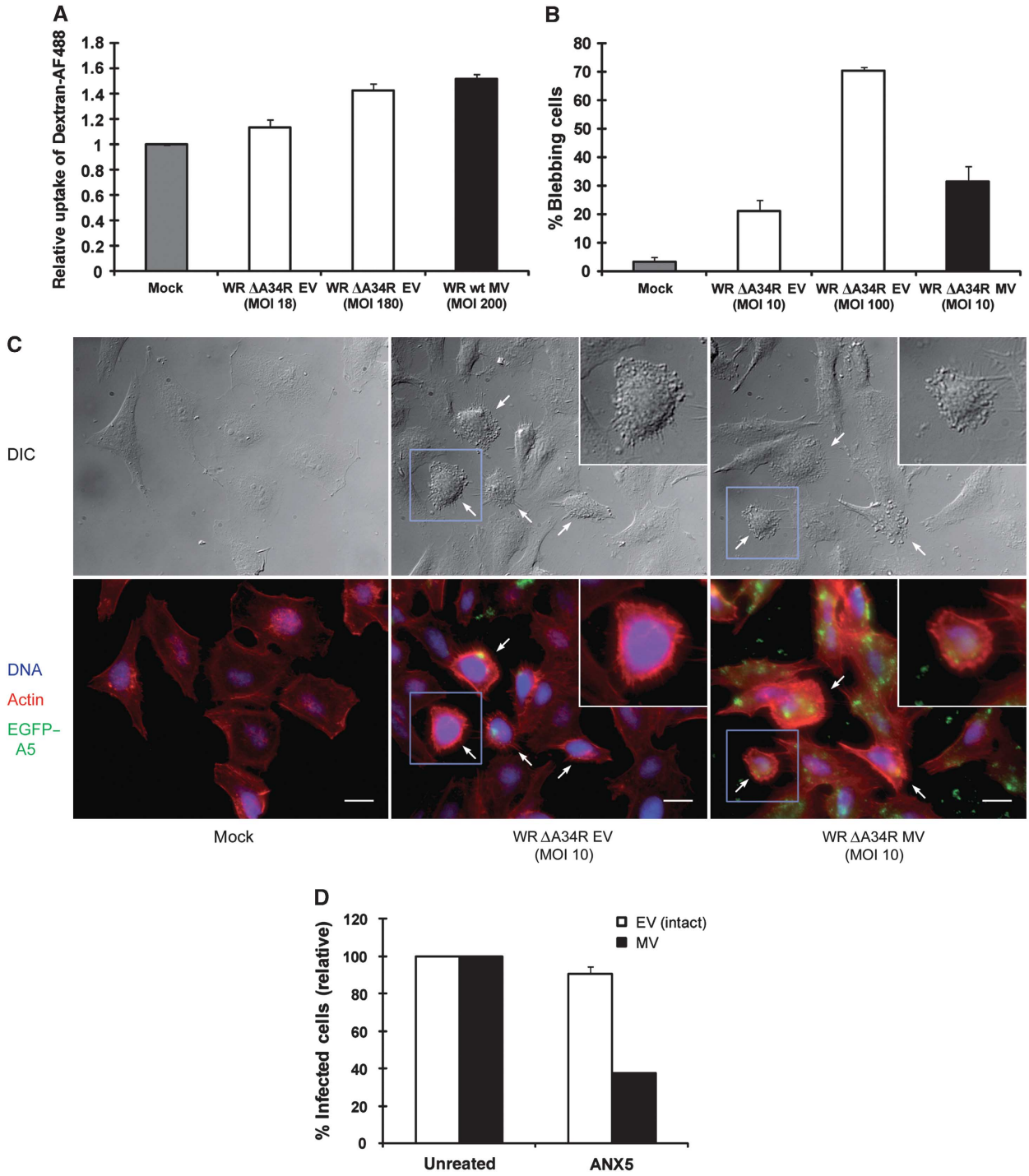

Figure 5 EVs and cellular phenotypes of macropinocytosis. (**A**) VAVC-induced fluid-phase uptake. WR ΔA34R EVs and WR wt MVs were bound to serum-starved HeLa cells on ice for 1.5 h and cells pulsed for 10 min at 37°C with 10 kDa dextran-AF 488. Cells were washed, harvested, fixed, and geometric means of green fluorescence quantified by flow cytometry. Dextran uptake was normalized to uptake by unstimulated cells and mean values ± s.e.m. of three independent experiments are shown. (**B**, **C**) VAVC-induced cell blebbing. WR ΔA34R EGFP–A5 MVs or concentrated EVs were bound to HeLa cells at room temperature (RT). Cells were incubated at 37°C for 40 min, fixed, stained, and analysed by DIC and wide-field fluorescence microscopy. The number of total and blebbing cells from three independent experiments (~250 cells per condition and experiment) was counted and mean ± s.e.m. is shown (**B**). Representative images are shown in (**C**). Scale bars = 20 μm. (**D**) WR ΔA34R infection—ANX5. Exposed PS of concentrated EVs or MVs of WR ΔA34R GFP (MOI 4) was masked with ANX5. Subsequently, virions were incubated at 37°C for 1 h (in case of EVs in the presence of 7D11) and used for infection experiments as described in Figure 4. Experiments were performed three times independently, mean values ± s.e.m. are shown.

EV infection requires acidification of endocytic vacuoles

Macropinocytosis leads to the uptake of fluid and particles into endocytic vacuoles that subsequently undergo acidification (Mercer and Helenius, 2009). To determine if low pH was needed for EV infection, we blocked acidification of endocytic organelles in HeLa cells using the vATPase inhibitor bafilomycin A1 (BafA) and the carboxylic ionophore monensin

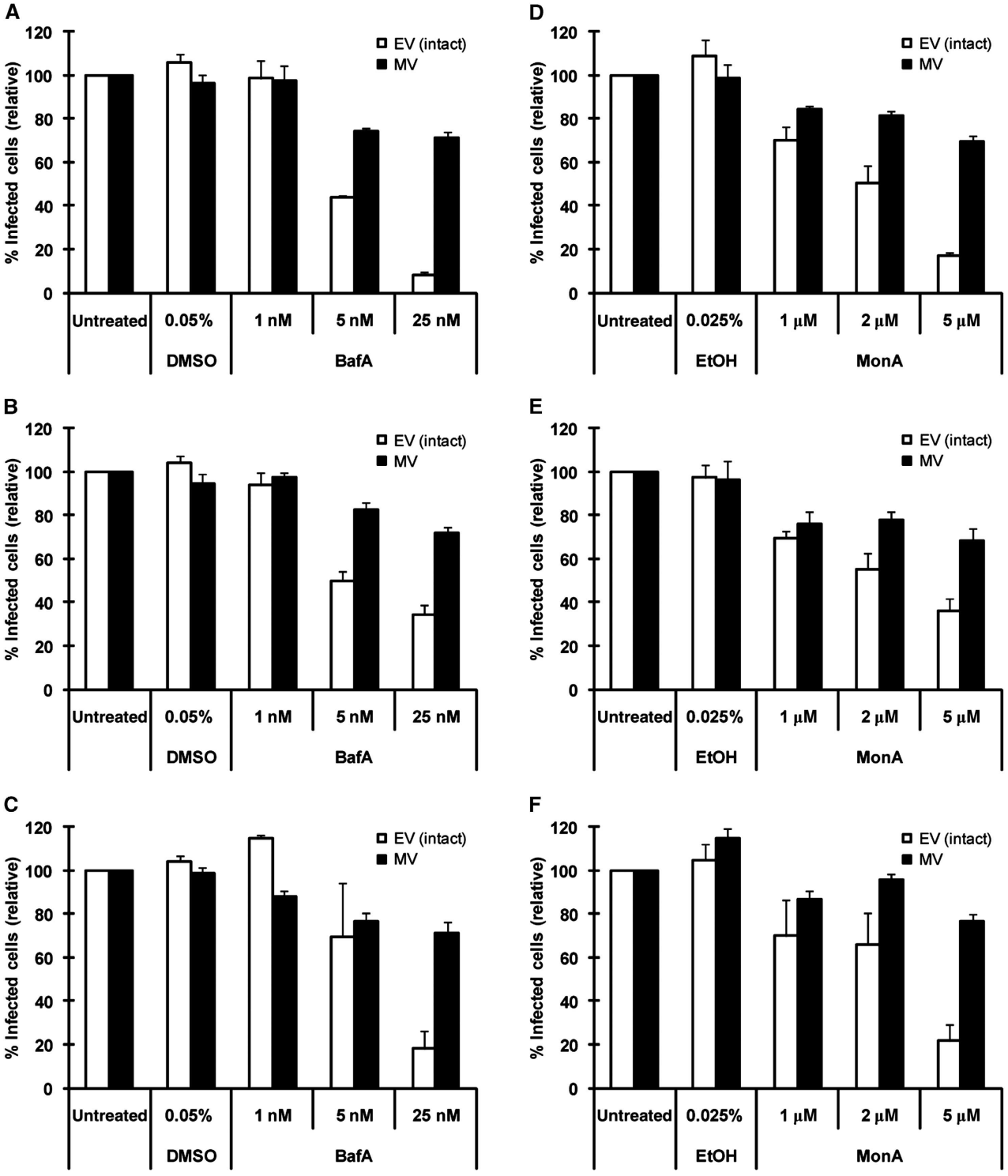

Figure 6 EV infection and acidification of endocytic vacuoles. Experimental setup as in Figure 4; HeLa cells were pretreated with BafA (**A**–**C**) or MonA (**D**–**F**) for 1 h; controls with solvents at the highest used concentrations were included. Infection with IHD-J GFP (**A**, **D**), WR GFP (**B**, **E**), or WR ΔA34R GFP (**C**, **F**) in the presence of drugs was quantified by flow cytometry; mean ± s.e.m. of three independent, normalized experiments are shown.

A (MonA) (Figure 6A–F). At concentrations that did not significantly affect infection by MVs, both compounds reduced EV infection in a dose-dependent manner. IHD-J and WR ΔA34R EV infection was reduced by 80% at the highest concentrations. WR EV infection was only reduced by up to 65%. Infection with IHD-J EVs was also blocked by BafA in several other cell lines including A549N, BSC-40, RK13, and Vero (data not shown).

Thus, acidification of endocytic vesicles was required for efficient infection by intact EVs, whereas MVs were less sensitive to the perturbants of vacuolar acidification at the concentrations used.

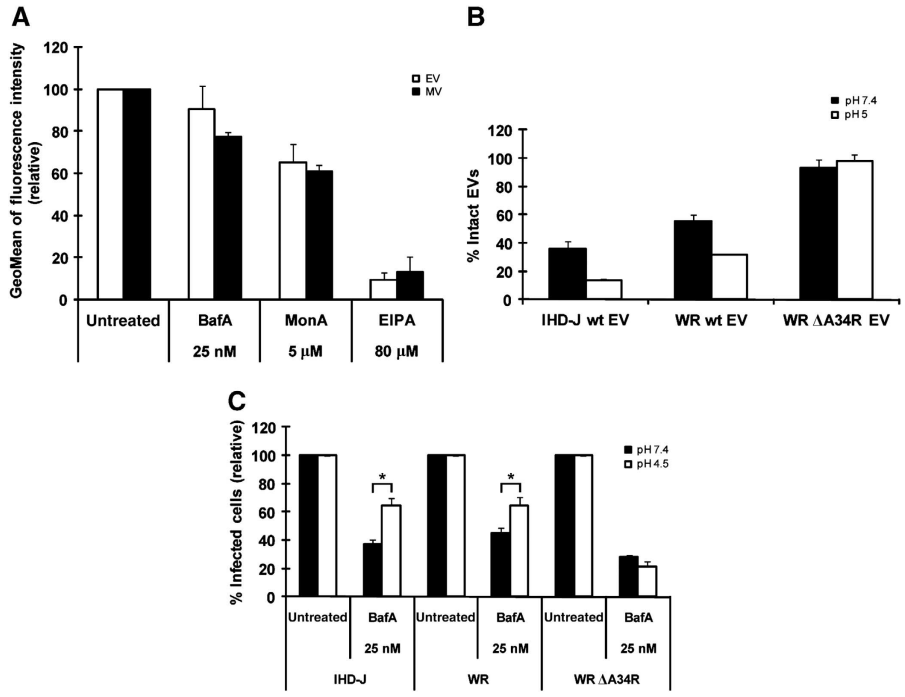

Figure 7 EV internalization and acid-mediated EV membrane disruption. (**A**) IHD-J—internalization. EV (IHD-J F13–GFP) and MV (IHD-J EGFP–A5) internalization in the presence of BafA, MonA, and EIPA was quantified as described in Figure 4B. (**B**) *In vitro* EV membrane disruption. IHD-J, WR, and WR ΔA34R EVs were incubated at pH 5.0 or pH 7.4 and 37°C for 5 min. EVs were titrated with or without 7D11 at pH 7.4 as described in Figure 1A. The percentage of intact EVs was calculated by normalizing plaque numbers after 7D11 neutralization to plaque numbers in untreated samples; mean values ± s.e.m. of three independent experiments are presented. (**C**) EV infection—acid bypass of BafA block. HeLa cells were left untreated or treated with BafA for 1 h. EVs of IHD-J GFP, WR GFP, or WR ΔA34R GFP were preincubated in the presence of drugs and 7D11 for 1 h at 37°C (MOI 2). Virus particles were bound to cells on ice. Cells were shifted to 37°C in pH 7.4 or pH 4.5 medium for 5 min and then incubated in full medium with drugs for 4 h. Infected cells were quantified by flow cytometry. The percentage of infected cells was normalized to the untreated samples. All experiments were performed three times independently, mean values ± s.e.m. are shown, asterisks mark significant differences ($P<0.05$).

Acidification has a role in EV membrane disruption

To determine which step(s) in the entry process required low pH, we quantified endocytic internalization of IHD-J EVs and MVs in the presence of BafA and MonA (Figure 7A). Internalization into EIPA-treated cells was used as a control. BafA did not affect EV or MV internalization. MonA reduced internalization moderately, and EIPA strongly. This suggested that the effect of BafA on infection occurred after EV internalization.

To determine if the BafA-sensitive intracellular step of EV entry involved disruption of the outer membrane of EVs in endocytic compartments, we first tested whether EV membranes could be disrupted by low pH treatment *in vitro* as previously reported (Vanderplasschen *et al*, 1998a). When supernatants containing IHD-J and WR EVs were incubated with pH 5 buffer at 37°C for 5 min, the fraction of 7D11-resistant intact EVs dropped by 62 and 42%, respectively (Figure 7B). The fraction of intact WR ΔA34R EVs was not significantly altered, suggesting that EV membranes of this mutant cannot be disrupted by low pH *in vitro*. When fluorescent EV particles of strain IHD-J mCherry–A5 F13–GFP were subjected to the same treatment and bound to cover slips, however, no significant loss of F13–GFP fluorescence was detected (data not shown), suggesting that disrupted EV membranes remained associated with the underlying virus particle.

The observed increase in 7D11 sensitivity upon low pH treatment suggested that the BafA-sensitive step of EV entry may involve rupture of the EV membrane within acidified endocytic compartments. If this were the case, infection in the presence of BafA might be rescued if EV membranes were artificially disrupted before internalization. To test this, 7D11-treated EVs were bound to HeLa cells in the cold and cells treated for 5 min at 37°C with pH 7.4 or pH 4.5 medium. Infection was quantified 4 h after treatment (Figure 7C).

After neutral or low pH treatment, infection of untreated cells with EVs of strains IHD-J (32 and 31%), and WR (20 and 20%) was similar (absolute data not shown). In BafA-treated cells, however, IHD-J and WR infection was increased by 72 and 43% in cells exposed to low pH when compared with controls. That acid-induced disruption of EV membranes partly rescued infection in cells with impaired macropinosomal acidification suggested that EV membrane disruption was indeed the step in EV entry that was inhibited by BafA. Infection with WR ΔA34R EVs in the presence of BafA was not increased after low pH treatment. This was consistent with the finding that low pH did not trigger disruption of the EV membrane of this strain *in vitro*.

If EV membrane disruption required acidification of endocytic vesicles, intact EV particles would be expected to accumulate in those compartments when acidification is inhibited by BafA. To test this, we infected HeLa cells with IHD-J mCherry–A5 F13–GFP EVs for 3 h in the absence or presence of BafA. Disrupted EVs were not neutralized with 7D11 in this experiment as they would accumulate in macropinosomes making them indistinguishable from accumulated intact EVs. To prevent early gene expression, which hampers microscopic analysis due to transient cell rounding, micro-

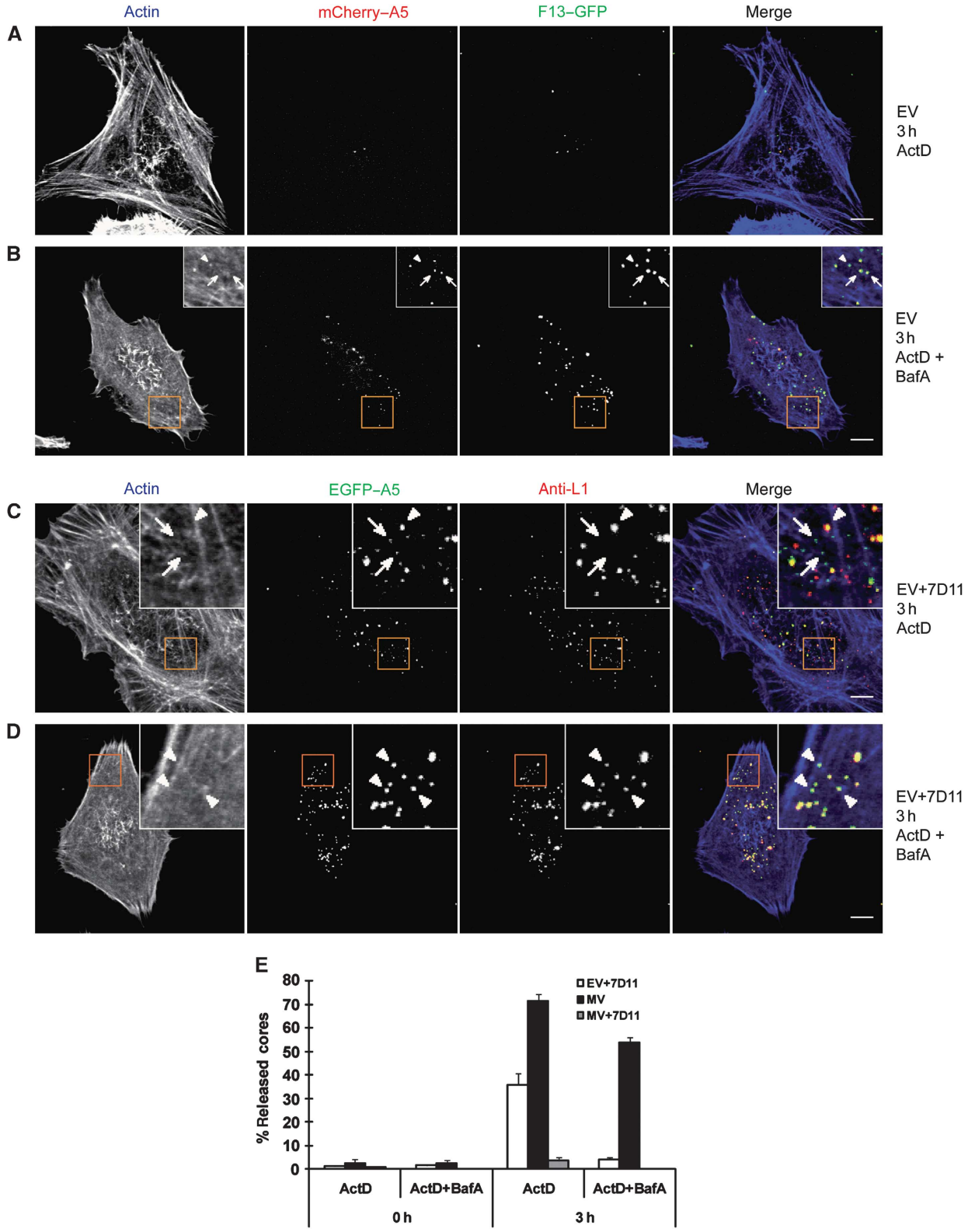

Figure 8 EV accumulation and core release in the presence of BafA. (**A**–**E**) HeLa cells were infected with IHD-J mCherry–A5 F13–GFP EVs (MOI 25) (**A**, **B**) or 7D11-treated IHD-J EGFP–A5 EVs (MOI 8 after 7D11 incubation) (**C**–**E**) in the presence of 5 μg/ml ActD and 25 nM BafA where indicated. Particles were bound to pretreated cells on ice and incubated in full DMEM with drugs at 37°C for 3 h. Samples were fixed and stained for actin (**A**, **B**) or L1 (Mab 7D11) and actin (**C**, **D**). (**A**–**D**) Images were recorded by confocal microscopy and representative maximum projections of *Z*-stacks are shown. Arrows in the insets of (**B**) highlight EVs, the arrowhead marks a free EV membrane. Arrows in the insets of (**C**, **D**) highlight released viral cores, arrowheads point at viral particles that were stained for the MV-membrane marker L1. Scale bars = 10 μm. (**E**) The percentage of released cores after infection with 7D11-treated EVs, MVs, and 7D11-treated MVs in the presence of the indicated drugs was quantified in three independent experiments. Controls with bound virus (0 h) were included. Core release from 7D11-neutralized MVs was only quantified in the presence of ActD. Mean values ± s.e.m. are shown.

scopy experiments were performed in the presence of actinomycin D (ActD) (typical cells shown in Figure 8A and B). Significantly more EVs were observed in cells infected in the presence of BafA (arrows B, inset) than in cells with unperturbed acidification. EV membranes without viral cores were also detected (filled arrowhead, inset). These may be the remnants of disrupted EVs, whose underlying MV-like particles underwent fusion. Viral cores containing mCherry-A5 that were released into the cytosol could not be reliably detected with our confocal microscopy setup. When bound EV particles were stained under non-permeabilizing conditions, we found that the majority of EV particles that had accumulated in the presence of BafA was internalized (Supplementary Figure S5).

If disruption of intact EVs is inhibited in the presence of BafA, it reasons that no MV-like particles would be exposed and, therefore, no viral cores could be released into the host cell cytosol by fusion. To analyse core release, we used IHD-J EGFP–A5 EVs and exploited that VACV cores accumulate in the presence of ActD (Pedersen *et al*, 2000). Using this approach, we detected and quantified the percentage of free viral cores within the cytoplasm 3 h after infection. To differentiate between viral cores released by fusion and viral particles in endocytic vesicles or bound to the cell (EVs, released MV-like particles, or MVs), virions were stained for the presence of the MV-membrane protein L1 (Figure 8C–E; Supplementary Figure S6). In addition, EVs were treated with 7D11 before infection, preventing any core release from disrupted EVs or contaminating MVs. Untreated MVs and MVs neutralized with 7D11 were used as controls. In the absence of BafA, 36% of the total cores in cells infected with intact EVs were released into the cytosol. In the presence of BafA, the percentage of free cores was reduced to 4%, indicating that BafA prevented release of EV-derived viral cores into the cytosol. MV core release was only moderately affected by BafA treatment, whereas MV neutralization with 7D11 almost completely abolished the release of cores.

Taken together, the results suggested that acidification of endocytic vacuoles was required for a step of EV entry after endocytic uptake and before release of viral cores. Since fusion of MVs was not inhibited by the concentration of BafA used, the acid-dependent step of EV entry is most likely the disruption of the EV membrane within endocytic compartments. This is further supported by the fact that artificial disruption of the EV membrane could bypass the need for low pH in endocytic vesicles and by the observation that EVs accumulated within BafA-treated cells.

Discussion

With this series of experiments, we aimed at characterizing the entry pathway of VACV EVs. We could show that EVs were rapidly internalized by endocytosis, and that the mechanism was virus-induced, macropinocytic, and essential for infection by intact EVs. We found that loss of the outer EV membrane occurred after endocytic internalization, and concluded that acidification of endocytic compartments was required for this step of EV entry. Presumably, as shown in the schematic view of the entry program in Figure 9, the inner membrane with the EFC was exposed after EV membrane rupture. It could then undergo fusion with the limiting membrane of the macropinosome, resulting in core release into the cytosol.

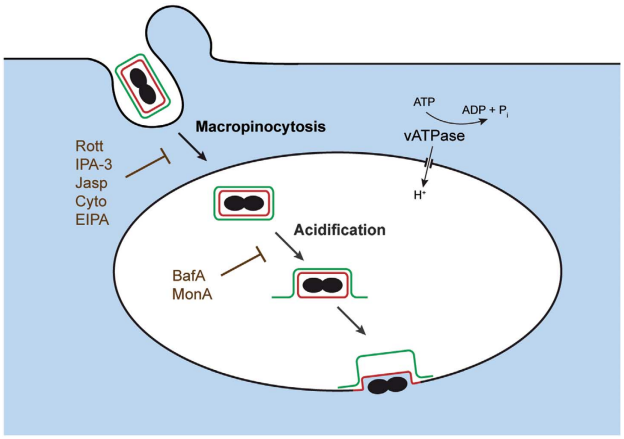

Figure 9 Mechanism of VACV EV entry. VACV EVs induce fluid-phase uptake by macropinocytosis and are internalized with the bulk fluid. The pH in macropinosomes decreases in the course of their maturation, which triggers disruption of the outer EV membrane. Exposed EFCs in the membrane of MV-like particles catalyse or regulate fusion with limiting endocytic membranes and thereby release virus cores with the genome into the cytosol allowing for successful replication.

Judging by the insensitivity to MAb 7D11, only a relatively small fraction (10–40%) of EVs released from VACV-infected RK13 cells and other cell types (data not shown) contained an intact outer membrane. Although previous studies have reported higher proportions of intact EVs (65–75%) (Ichihashi, 1996; Vanderplasschen *et al*, 1998a; Law *et al*, 2006; Benhnia *et al*, 2009), it is evident that many of the EVs released from cells possess outer membranes that are not fully sealed (Husain *et al*, 2007). Although we could occasionally detect free outer membranes in our preparations, the ruptured EV membranes typically remained associated with the particles. Rupture of the EV membranes did not affect the virus infectivity, but it made them susceptible to antibodies against MV antigens.

Using fluorescence and electron microscopy, we could show that EVs were internalized into HeLa cells before loss of their outer membrane. In the fluorescence microscopy experiments, we used recombinant viruses in which the core and the EV membrane were visualized by different fluorescent proteins. By EM, we could identify intravacuolar virus particles with two membranes resolved, and with immunolabelling of GFP fused to the outer membrane protein F13. The internalization of EVs could also be confirmed by flow cytometry.

The mechanism of endocytosis used by EVs to enter cells was studied using a set of pharmacological inhibitors known to block endocytic processes (Mercer and Helenius, 2009). It was found that EV infection was dependent on EGFR, PKC, smMLCK, PAK1, actin dynamics, and sodium–proton exchangers. It was not affected by staurosporin, Geni, and Wort, three kinase inhibitors known to inhibit various endocytic mechanisms. Taken together, the inhibitor profile strongly suggested that infection by intact EVs involved macropinocytosis (Mercer and Helenius, 2009). We could furthermore show that internalization of EVs was blocked by inhibitors of PAK1, actin dynamics, and sodium–proton exchangers, and observed EVs in intracellular vesicles positive for the fluid-phase marker dextran. Macropinocytic uptake was confirmed by experiments using WR ΔA34R, a mutant virus

producing almost exclusively intact EVs. It was found to induce an MV-independent elevation in fluid-phase uptake and induced PM ruffling in the form of blebs.

A role for macropinocytosis was consistent with a recent report showing that MV and EV internalization, as well as early gene expression, in monocyte-derived DCs depends on macropinocytosis (Sandgren *et al*, 2010). However, the authors only visualized uptake of viral cores and did not follow the fate of EV membranes. Furthermore, DCs unlike most other cell types maintain ongoing, constitutive macropinocytosis without the requirement for external triggers (Sallusto *et al*, 1995; Norbury *et al*, 1997; Norbury, 2006). This is part of their function as immune cells responsible for antigen capture and presentation. In other cell types, including the HeLa cells used here, macropinocytosis is a transient, ligand-triggered process (Mercer and Helenius, 2009). Thus, our data showed a role for macropinocytosis in cell lines that do not undergo continuous, constitutive macropinocytosis. For productive infection of HeLa cells, EVs apparently induced the complete program of macropinocytosis starting with signal transduction, PM blebbing, and increased fluid uptake.

That MVs are also internalized by macropinocytosis has been recently shown with a variety of virus strains and cell types (Huang *et al*, 2008; Mercer and Helenius, 2008; Laliberte and Moss, 2009; Mercer *et al*, 2010; Moser *et al*, 2010). This is perhaps not surprising considering that EVs and MVs might be excluded from most other endocytic pathways in non-phagocytic cells due to their size. However, the mechanism of macropinocytosis induction was likely to be different for the two particle types as they do not contain common viral proteins on the surface and there is no evidence for common cellular components. In contrast to MV infection, EV infection was not inhibited by the PS-binding protein ANX5. Evidently, EVs did not share the apoptotic mimicry mechanism employed by MVs (Mercer and Helenius, 2008). The requirement for macropinocytosis is, however, shared with a number of virus families including herpes- and filoviruses for which the mechanism of triggering is not clear (Coyne *et al*, 2007; Amstutz *et al*, 2008; Karjalainen *et al*, 2008; Raghu *et al*, 2009; Kalin *et al*, 2010; Nanbo *et al*, 2010; Saeed *et al*, 2010). Macropinocytosis as a cellular mechanism is a potential drug target for new antiviral agents.

The effect of BafA and MonA showed that EV-induced infection of HeLa cells required organelle acidification. While internalization was not inhibited by BafA, the drug prevented the release of viral cores from intact EVs. That disruption of the outer EV membrane barrier within endocytic vesicles was the affected step was supported by several observations. First, we confirmed previous reports that the EV membrane is sensitive to low pH *in vitro* (Ichihashi, 1996; Vanderplasschen *et al*, 1998a). Second, we observed that artificial disruption of the EV membrane partially rescued infection in the presence of BafA. Third, we found that infection with EV suspensions in the absence of MAb 7D11 (containing 60–90% disrupted EVs) was significantly less sensitive to BafA or MonA (data not shown). Fourth, EVs with both membranes accumulated intracellularly in the presence of BafA. Fifth, release of viral cores from MVs was not inhibited by the utilized BafA concentrations, suggesting that fusion was not affected. MV-like particles wrapped in the EV membrane differ from MVs in that they lack A26 (Ulaeto *et al*, 1996). MVs of VACV strains lacking A26 were capable of fusing at neutral pH in conditions in which MV infection was sensitive to BafA (Chang *et al*, 2010), strengthening the conclusion that fusion of MV-like particles is insensitive to BafA. Although low pH seemed essential for EV disruption, we cannot exclude the possibility that the interaction with glycosaminoglycan (GAG) chains contributes to disruption as previously suggested (Law *et al*, 2006). However, when the murine cell line L and its GAG-deficient derivative sog9 (Banfield *et al*, 1995) were infected with IHD-J or WR EVs, infection levels in both cell lines were similar, suggesting that GAGs were not required for efficient EV infection. Inhibition of EV infection by BafA was similar in L and sog9 cells (data not shown).

The mutant WR ΔA34R is interesting because the outer membrane of its EVs is not as susceptible to disruption by GAG chains (Law *et al*, 2006) and low pH (Figure 7B) as that of wild-type virus. EVs of this virus lack the EV membrane protein A34 and incorporate reduced amounts of two other EV membrane proteins, B5 and A33 (Earley *et al*, 2008; Perdiguero *et al*, 2008). Acidic residues in the membrane-proximal stalk region of B5 are required for GAG-triggered EV disruption (Roberts *et al*, 2009), and it is possible that both GAG- and low pH-mediated EV rupture share a mechanism that depends on B5 and A34. That WR ΔA34R EVs are infectious despite their resistance to low pH-mediated disruption implies that loss of the outer membrane can be triggered by other mechanisms. Nevertheless, infection remained sensitive to acidification inhibitors, suggesting a need for WR ΔA34R EVs to pass through acidified endocytic compartments for productive infection.

The immune system of poxvirus-infected organisms is challenged by two distinct infectious entities, EVs and MVs, that expose no common epitopes. The outer EV membrane serves as a protective shield under which an MV-like particle can hide during virus spread through body fluids. Consistent with such a role, the EV membrane contains complement control proteins (Vanderplasschen *et al*, 1998b), and EVs are more difficult to neutralize with antibodies than MVs (Law and Smith, 2001). The key viral proteins involved in membrane fusion remain hidden and protected until needed. The cue for disruption of the outer EV membrane is the low pH, which the virus is likely to encounter for the first time in the macropinosome. Our results thus indicate that the protective outer membrane of an incoming EV is shed at the latest possible time point, that is when the virus has been internalized and is no longer accessible to extracellular factors.

Materials and methods

Cell lines

BSC-40 (African green monkey) and HeLa (human) cells were cultivated in DMEM (Gibco BRL) supplemented with 10% heat-inactivated FCS, glutamax, and penicillin–streptomycin; for BSC-40 cells non-essential amino acids and sodium pyruvate were added as well; RK13 (rabbit) cells were cultivated in MEM (Gibco BRL) supplemented with 10% heat-inactivated FCS, glutamax, non-essential amino acids, penicillin–streptomycin, and sodium pyruvate.

Viruses

Recombinant VACVs were generated based on VACV strain WR, VACV WR ΔA34R (a kind gift of Bernard Moss, NIH, Bethesda, MD,

USA) (Wolffe *et al*, 1997), and VACV strain IHD-J as previously described (Mercer and Helenius, 2008). Briefly, GFP-expressing strains were generated using vectors based on the plasmid pJS4 (Chakrabarti *et al*, 1997). Strains encoding EGFP–A5 or mCherry–A5 in the endogenous locus were constructed using vectors based on pBluescript II KS (Fermentas, St Leon-Rot, Germany) bearing the EGFP or mCherry coding sequence flanked by the respective VACV WR genomic regions. VACV strains expressing F13–GFP were a kind gift of Rafael Blasco (INIA, Madrid, Spain) (Geada *et al*, 2001). To build strains encoding both mCherry–A5 and F13–GFP, BSC-40 cells were co-infected with mCherry–A5 and F13–GFP viruses; dual-coloured recombinants of the parental viruses were selected through four rounds of plaque purification on BSC-40 cells.

MV particles were produced in BSC-40 cells and purified from cytoplasmic lysates as described elsewhere (Mercer and Helenius, 2008). EV particles were produced in RK13 cells and collected from the supernatant. Confluent tissue culture flasks were infected with the respective MVs in serum-free medium at an MOI of 1 for 1 h. Cells were washed with PBS and overlayed with full medium. At 24 h after infection, supernatants were collected and loose cells were sedimented by two low speed centrifugation steps (400 *g*, 10 min, 4°C). EV-containing supernatants were either used directly or concentrated by sedimentation (40 min, 38 000 *g*, 4°C) and resuspended in full or serum-free medium.

Antibodies

Hybridoma cells to produce the mouse MAb 7D11 (anti-L1) (Wolffe *et al*, 1995) were kindly provided by Bernard Moss with permission of Alan Schmaljohn (University of Maryland, Baltimore, MA, USA). MAbs were purified from hybridoma supernatants by BioGenes (Berlin, Germany). MAb VMC-20 (anti-B5) from ascites fluid was a kind gift of Roselyn J Eisenberg and Gary H Cohen (University of Pennsylvania, Philadelphia, PA, USA) (Aldaz-Carroll *et al*, 2005). Rabbit polyclonal anti-GFP was purchased from Rockland (Gilbertsville, PA, USA). Fluorophore-coupled goat anti-mouse secondary antibodies were obtained from Invitrogen (Carlsbad, CA, USA).

Drugs and reagents

ActD, BafA, CalC, Cyto, Chlo, EIPA, IPA-3, Geni, ML-7, MonA, Rott, Stau, and Wort were obtained from Sigma-Aldrich; Jasp was purchased from Enzo Life Sciences (Farmingdale, NY, USA) and Iressa from LC laboratories (Woburn, MA, USA); AF 594-coupled phalloidin (Invitrogen) was used for actin staining, Draq5 (Biostatus, Shepshed, UK) for DNA staining.

EV plaque assay

To assay the fraction of intact infectious EVs, virus samples were incubated with or without 5 μg/ml MAb 7D11 at 37°C for 1.5 h. Serial dilutions were prepared and 50 μl of each was added to confluent BSC-40 cells in six-wells covered with 1 ml DMEM. After 1 h at 37°C, cells were washed with 1 ml PBS and overlayed with 2 ml full DMEM (WR) or full DMEM with 1.5% carboxymethyl cellulose (IHD-J). Cells were stained after 48–72 h (0.1% crystal violet, 2% formaldehyde in H_2O).

Microscopic analysis of EV particles

The integrity of EVs on the particle level was analysed using confocal microscopy. EV particles of strain IHD-J mCherry–A5 F13–GFP from clarified supernatants were incubated with 5 μg/ml MAb 7D11 at 37°C for 1 h and bound to cover slips. Samples were fixed with formaldehyde and stained with AF 647 goat anti-mouse. *Z*-stacks were recorded using a Zeiss LSM510 Meta confocal system. Particles were detected using the ImageJ particle detector and tracker plugin (Sbalzarini and Koumoutsakos, 2005) on *Z* projections (radius = 3, cutoff = 0, percentile 0.07 (green)/0.1 (blue)/0.05 (red)) and coordinates were compared with a custom-written Matlab program (distance cutoff >3 pixels (540 nm)).

Confocal microscopy internalization experiment

To assay the internalization of EVs, IHD-J EV particles (3× concentrated supernatants) were bound to HeLa cells on cover slips for 1 h on ice. Cells were either stained directly or incubated in full medium at 37°C for 30 min. Cells were cooled down, washed, and incubated with VMC-20 (1:10 000 in PBS/1% BSA) on ice for 2 h. Cells were fixed and stained with AF 647 goat anti-mouse and AF 594 phalloidin (where indicated). Control samples were fixed and permeabilized before staining. *Z*-stacks were recorded using a Zeiss LSM510 Meta confocal system.

Electron microscopy internalization experiment

To visualize internalized EVs, IHD-J F13–GFP EV particles (60× concentrated supernatants) were bound to HeLa cells on ice for 1 h. Cells were incubated in full medium at 37°C for 30 min, and fixed in 4% formaldehyde and 0.1% glutaraldehyde in 1× PHEM buffer (Schliwa *et al*, 1981) for 90 min. Cryosectioning and immunolabelling was performed as described elsewhere (Tokuyasu, 1973; Slot and Geuze, 2007). In brief, ultrathin sections (50–70 nm) from gelatin-embedded and frozen cell pellets were obtained using an FC7/UC7-ultramicrotome (Leica, Vienna, Austria).

Immunogold labelling was carried out on thawed sections with anti-GFP antibodies (1:200) and 10 nm protein A-gold (UMC Utrecht University, Utrecht, The Netherlands) (1:50); a mixture of uranyl acetate and methyl cellulose was used for embedding and negative staining. Sections were examined with a CM10 Philips transmission electron microscope with an Olympus 'Veleta' $2k \times 2k$ side-mounted TEM CCD camera.

Flow cytometry internalization assay

Subconfluent 12-wells of HeLa cells were used for flow cytometry-based internalization assays. Cells were pretreated with inhibitors for 15–60 min in full DMEM; EVs (IHD-J F13–GFP, 0.25 ml 35× concentrated supernatants) or MVs (IHD-J EGFP–A5, 7.5×10^7 p.f.u. in 0.25 ml) in serum-free medium were bound to cells on ice for 1 h. Cells were washed and incubated with full medium (+inhibitors) at 37 or 0°C for 30 min. Cells were washed with PBS and incubated with 0.25% Trypsin/EDTA at 37°C for 10 min to detach cells and remove bound virus. Alternatively, cells were detached with 1 mM EDTA/PBS at 0°C for 30 min. Cells were resuspended and washed in 7% FCS in PBS, fixed and analysed using a Becton Dickinson (BD) FACSCalibur flow cytometer and the FlowJo software package.

Flow cytometry infection assay

Confluent 12-wells of HeLa cells were infected for flow cytometry-based infection assays. Pretreatment with inhibitors was performed for 15–60 min in full MEM (as used for RK13 cells and present in EV supernantants). MVs (2×10^6 p.f.u. in 0.5 ml) and EVs (0.5 ml EV supernatant or concentrate) were prepared in full MEM (+inhibitors). Disrupted EVs and contaminating MVs in the EV samples were neutralized with 5 μg/ml 7D11 for 1 h at 37°C and added to cells. After 30 min at 37°C, cells were washed and overlayed with 1 ml full MEM (+inhibitors). Four hours after infection, cells were prepared for flow cytometry. Cells were analysed using a BD FACSCalibur flow cytometer and the BD CellQuest Pro software or the FlowJo software package.

Fluid-phase uptake assay

Virus-induced fluid-phase uptake was quantified as described previously (Meier *et al*, 2002). Subconfluent HeLa cells in 24-well plates were serum starved in 0.2% BSA/DMEM for 4 h. WR wt MVs or WR ΔA34R EVs in 0.2% BSA/RPMI were then bound to the cells in the cold for 90 min. Cells were washed and pulsed for 10 min at 37°C with 0.5 mg/ml 10 kDa dextran-AF 488 (Invitrogen) in RPMI/BSA. Cells were washed with BSA/RPMI, PBS (2×), 100 mM NaOAc (pH 5.5)/50 mM NaCl, and PBS. Cells were detached with 0.25% trypsin (25 min on ice, 1 min at RT), resuspended with 7% FCS in PBS and fixed in 4% formaldehyde over night at 4°C. Fluorescence of cells was quantified using a BD FACSCalibur flow cytometer and the FlowJo software package.

Blebbing assay

To quantify the induction of blebbing, HeLa cells were grown on cover slips to 50% confluency. MV or EV suspensions (0.5 ml) of WR ΔA34R EGFP–A5 in 2% BSA/PBS were added to cells at RT for 1 h. Cells were washed and incubated with full medium at 37°C for 40 min. Samples were fixed with 4% formaldehyde at RT, and DNA and actin stained with Draq5 and AF 594 phalloidin. Microscopy images were recorded using an Olympus Cell^R imaging station with DIC setup. Total and blebbing cells were counted manually ($n_{total} \sim 250$ cells/condition and experiment).

Annexin V binding

Exposed PS on virion membranes was masked with ANX5 to test the requirement of PS on infection. A modified version of the

manufacturer's protocol (Vybrant® Apoptosis Assay kit #2; Molecular Probes) was used for labelling. In brief, sedimented virions were washed twice with ANX5-binding buffer (10 mM Hepes, 140 mM NaCl, 2.5 mM $CaCl_2$, pH 7.4), resuspended in 200 µl ANX5-binding buffer and split into two samples. Samples were left untreated or treated with 20 µl AF 647 ANX5 for 1 h at RT. Virions were washed twice with ANX5-binding buffer, resuspended in DMEM and used for infection experiments.

EV disruption

To disrupt EV particles *in vitro*, 20 µl EVs (clarified supernatant of infected RK13 cells) were mixed with 180 µl 10 mM Na-citrate (pH 5.0), incubated at 37°C for 5 min and neutralized with 100 µl 1 M Hepes pH 7.4. For controls, Hepes was added to virus samples premixed with low pH buffer. Integrity of EVs was quantified by plaque assay as described above.

To rescue infection by low pH treatment, 7D11-treated EV particles were bound to drug-treated HeLa cells on ice for 1 h in the presence of drugs. Cells were incubated for 5 min with full DMEM containing 30 mM MES (pH 4.5) or full DMEM (pH 7.4) at 37°C. Cells were washed twice and treated as described in the flow cytometry infection assay. SigmaPlot (Systat software) was used to compare sample groups by *t*-test.

Core release assay

To detect and quantify viral cores, HeLa cells on cover slips were pretreated with inhibitors in full DMEM for 30 min. IHD-J EGFP–A5 EVs (0.25 ml 4× concentrated EV supernatant) or MVs (1.3×10^7 p.f.u. in 0.25 ml) in 2% BSA/PBS were pretreated with or without 5 µg/ml 7D11 for 1 h at 37°C. Virions were bound to cells on ice for 1 h in the presence of drugs. Cells were washed with PBS and incubated in full medium with drugs for 3 h. Cells were fixed with formaldehyde, and stained with 7D11 (540 ng/ml)/AF 594 goat anti-mouse and AF 647 phalloidin. *Z*-stacks were recorded using a Zeiss LSM510 Meta confocal system. Green fluorescent cores were detected with the spot detection function of Imaris (Bitplane) using the quality parameter. Detected spots with a mean green intensity <20 were omitted and spots with a mean red fluorescent intensity <50 were classified as released cores ($n_{total} \sim 750$ cores in 10 cells/condition and experiment).

Supplementary data

Supplementary data are available at *The EMBO Journal* Online (http://www.embojournal.org).

Acknowledgements

We thank Veronika Graml for help with image analysis, Stefan Kälin for help with dextran uptake experiments, and the Light Microscopy Center (LMC), ETH Zürich, for microscopy support. We are grateful to Lucia Reh, Andrea Rothballer, and Yohei Yamauchi for critical reading of the manuscript. This work was in part funded by grants from EMBO, ETH Zurich, and the Swiss National Foundation (InfectX, Sinergia). FIS was supported by a Boehringer Ingelheim PhD fellowship.

Author contributions: FIS, CKB, and JPM performed the experiments; FIS, CKB, AH, and JM analysed the data; FIS, AH, and JM conceived and designed the experiments; FIS, AH, and JM wrote the manuscript.

Conflict of interest

The authors declare that they have no conflict of interest.

References

Aldaz-Carroll L, Whitbeck JC, Ponce de Leon M, Lou H, Hirao L, Isaacs SN, Moss B, Eisenberg RJ, Cohen GH (2005) Epitope-mapping studies define two major neutralization sites on the vaccinia virus extracellular enveloped virus glycoprotein B5R. *J Virol* **79:** 6260–6271

Amstutz B, Gastaldelli M, Kalin S, Imelli N, Boucke K, Wandeler E, Mercer J, Hemmi S, Greber UF (2008) Subversion of CtBP1-controlled macropinocytosis by human adenovirus serotype 3. *EMBO J* **27:** 956–969

Banfield BW, Leduc Y, Esford L, Schubert K, Tufaro F (1995) Sequential isolation of proteoglycan synthesis mutants by using herpes simplex virus as a selective agent: evidence for a proteoglycan-independent virus entry pathway. *J Virol* **69:** 3290–3298

Benhnia MR, McCausland MM, Moyron J, Laudenslager J, Granger S, Rickert S, Koriazova L, Kubo R, Kato S, Crotty S (2009) Vaccinia virus extracellular enveloped virion neutralization *in vitro* and protection *in vivo* depend on complement. *J Virol* **83:** 1201–1215

Chakrabarti S, Sisler JR, Moss B (1997) Compact, synthetic, vaccinia virus early/late promoter for protein expression. *Biotechniques* **23:** 1094–1097

Chang SJ, Chang YX, Izmailyan R, Tang YL, Chang W (2010) Vaccinia virus A25 and A26 proteins are fusion suppressors for mature virions and determine strain-specific virus entry pathways into HeLa, CHO-K1, and L cells. *J Virol* **84:** 8422–8432

Coyne CB, Shen L, Turner JR, Bergelson JM (2007) Coxsackievirus entry across epithelial tight junctions requires occludin and the small GTPases Rab34 and Rab5. *Cell Host Microbe* **2:** 181–192

Cyrklaff M, Risco C, Fernandez JJ, Jimenez MV, Esteban M, Baumeister W, Carrascosa JL (2005) Cryo-electron tomography of vaccinia virus. *Proc Natl Acad Sci USA* **102:** 2772–2777

Damon IK (2007) Poxviruses. In *Fields Virology*, Knipe DM, Howley PM (ed), Vol. 5th, 75, pp 2947. Philadelphia: Lippincott-Raven

Davies SP, Reddy H, Caivano M, Cohen P (2000) Specificity and mechanism of action of some commonly used protein kinase inhibitors. *Biochem J* **351:** 95–105

Earley AK, Chan WM, Ward BM (2008) The vaccinia virus B5 protein requires A34 for efficient intracellular trafficking from the endoplasmic reticulum to the site of wrapping and incorporation into progeny virions. *J Virol* **82:** 2161–2169

Geada MM, Galindo I, Lorenzo MM, Perdiguero B, Blasco R (2001) Movements of vaccinia virus intracellular enveloped virions with GFP tagged to the F13L envelope protein. *J Gen Virol* **82:** 2747–2760

Gschwendt M, Muller HJ, Kielbassa K, Zang R, Kittstein W, Rincke G, Marks F (1994) Rottlerin, a novel protein kinase inhibitor. *Biochem Biophys Res Commun* **199:** 93–98

Hollinshead M, Vanderplasschen A, Smith GL, Vaux DJ (1999) Vaccinia virus intracellular mature virions contain only one lipid membrane. *J Virol* **73:** 1503–1517

Huang CY, Lu TY, Bair CH, Chang YS, Jwo JK, Chang W (2008) A novel cellular protein, VPEF, facilitates vaccinia virus penetration into HeLa cells through fluid phase endocytosis. *J Virol* **82:** 7988–7999

Husain M, Weisberg AS, Moss B (2007) Resistance of a vaccinia virus A34R deletion mutant to spontaneous rupture of the outer membrane of progeny virions on the surface of infected cells. *Virology* **366:** 424–432

Ichihashi Y (1996) Extracellular enveloped vaccinia virus escapes neutralization. *Virology* **217:** 478–485

Ichihashi Y, Oie M (1983) The activation of vaccinia virus infectivity by the transfer of phosphatidylserine from the plasma membrane. *Virology* **130:** 306–317

Kalin S, Amstutz B, Gastaldelli M, Wolfrum N, Boucke K, Havenga M, DiGennaro F, Liska N, Hemmi S, Greber UF (2010) Macropinocytotic uptake and infection of human epithelial cells with species B2 adenovirus type 35. *J Virol* **84:** 5336–5350

Karjalainen M, Kakkonen E, Upla P, Paloranta H, Kankaanpaa P, Liberali P, Renkema GH, Hyypia T, Heino J, Marjomaki V (2008) A Raft-derived, Pak1-regulated entry participates in alpha2beta1 integrin-dependent sorting to caveosomes. *Mol Biol Cell* **19:** 2857–2869

Kayali AG, Austin DA, Webster NJ (2002) Rottlerin inhibits insulin-stimulated glucose transport in 3T3-L1 adipocytes by uncoupling mitochondrial oxidative phosphorylation. *Endocrinology* **143:** 3884–3896

Laliberte JP, Moss B (2009) Appraising the apoptotic mimicry model and the role of phospholipids for poxvirus entry. *Proc Natl Acad Sci USA* **106:** 17517–17521

Law M, Carter GC, Roberts KL, Hollinshead M, Smith GL (2006) Ligand-induced and nonfusogenic dissolution of a viral membrane. *Proc Natl Acad Sci USA* **103:** 5989–5994

Law M, Smith GL (2001) Antibody neutralization of the extracellular enveloped form of vaccinia virus. *Virology* **280:** 132–142

Locker JK, Kuehn A, Schleich S, Rutter G, Hohenberg H, Wepf R, Griffiths G (2000) Entry of the two infectious forms of vaccinia virus at the plasma membrane is signaling-dependent for the IMV but not the EEV. *Mol Biol Cell* **11:** 2497–2511

Marsh M, Helenius A (2006) Virus entry: open sesame. *Cell* **124:** 729–740

Meier O, Boucke K, Hammer SV, Keller S, Stidwill RP, Hemmi S, Greber UF (2002) Adenovirus triggers macropinocytosis and endosomal leakage together with its clathrin-mediated uptake. *J Cell Biol* **158:** 1119–1131

Mercer J, Helenius A (2008) Vaccinia virus uses macropinocytosis and apoptotic mimicry to enter host cells. *Science* **320:** 531–535

Mercer J, Helenius A (2009) Virus entry by macropinocytosis. *Nat Cell Biol* **11:** 510–520

Mercer J, Knebel S, Schmidt FI, Crouse J, Burkard C, Helenius A (2010) Vaccinia virus strains use distinct forms of macropinocytosis for host-cell entry. *Proc Natl Acad Sci USA* **107:** 9346–9351

Moser TS, Jones RG, Thompson CB, Coyne CB, Cherry S (2010) A kinome RNAi screen identified AMPK as promoting poxvirus entry through the control of actin dynamics. *PLoS Pathog* **6:** e1000954

Moss B (2006) Poxvirus entry and membrane fusion. *Virology* **344:** 48–54

Moss B (2007) Poxviridae: the viruses and their replication. In *Fields Virology*, Knipe DM, Howley PM (ed), Vol. 5th, 74, pp 2906 Philadelphia: Lippincott-Raven

Nanbo A, Imai M, Watanabe S, Noda T, Takahashi K, Neumann G, Halfmann P, Kawaoka Y (2010) Ebolavirus is internalized into host cells via macropinocytosis in a viral glycoprotein-dependent manner. *PLoS Pathog* **6:** e1001121

Norbury CC (2006) Drinking a lot is good for dendritic cells. *Immunology* **117:** 443–451

Norbury CC, Chambers BJ, Prescott AR, Ljunggren HG, Watts C (1997) Constitutive macropinocytosis allows TAP-dependent major histocompatibility complex class I presentation of exogenous soluble antigen by bone marrow-derived dendritic cells. *Eur J Immunol* **27:** 280–288

Payne L (1978) Polypeptide composition of extracellular enveloped vaccinia virus. *J Virol* **27:** 28–37

Payne LG (1979) Identification of the vaccinia hemagglutinin polypeptide from a cell system yielding large amounts of extracellular enveloped virus. *J Virol* **31:** 147–155

Payne LG (1980) Significance of extracellular enveloped virus in the *in vitro* and *in vivo* dissemination of vaccinia. *J Gen Virol* **50:** 89–100

Pedersen K, Snijder EJ, Schleich S, Roos N, Griffiths G, Locker JK (2000) Characterization of vaccinia virus intracellular cores: implications for viral uncoating and core structure. *J Virol* **74:** 3525–3536

Perdiguero B, Lorenzo MM, Blasco R (2008) Vaccinia virus A34 glycoprotein determines the protein composition of the extracellular virus envelope. *J Virol* **82:** 2150–2160

Raghu H, Sharma-Walia N, Veettil MV, Sadagopan S, Chandran B (2009) Kaposi's sarcoma-associated herpesvirus utilizes an actin polymerization-dependent macropinocytic pathway to enter human dermal microvascular endothelial and human umbilical vein endothelial cells. *J Virol* **83:** 4895–4911

Roberts KL, Breiman A, Carter GC, Ewles HA, Hollinshead M, Law M, Smith GL (2009) Acidic residues in the membrane-proximal stalk region of vaccinia virus protein B5 are required for glycosaminoglycan-mediated disruption of the extracellular enveloped virus outer membrane. *J Gen Virol* **90:** 1582–1591

Saeed MF, Kolokoltsov AA, Albrecht T, Davey RA (2010) Cellular entry of ebola virus involves uptake by a macropinocytosis-like mechanism and subsequent trafficking through early and late endosomes. *PLoS Pathog* **6:** e1001110

Sallusto F, Cella M, Danieli C, Lanzavecchia A (1995) Dendritic cells use macropinocytosis and the mannose receptor to concentrate macromolecules in the major histocompatibility complex class II compartment: downregulation by cytokines and bacterial products. *J Exp Med* **182:** 389–400

Sandgren KJ, Wilkinson J, Miranda-Saksena M, McInerney GM, Byth-Wilson K, Robinson PJ, Cunningham AL (2010) A differential role for macropinocytosis in mediating entry of the two forms of vaccinia virus into dendritic cells. *PLoS Pathog* **6:** e1000866

Sbalzarini IF, Koumoutsakos P (2005) Feature point tracking and trajectory analysis for video imaging in cell biology. *J Struct Biol* **151:** 182–195

Schliwa M, Euteneuer U, Bulinski JC, Izant JG (1981) Calcium lability of cytoplasmic microtubules and its modulation by microtubule-associated proteins. *Proc Natl Acad Sci USA* **78:** 1037–1041

Senkevich TG, Ojeda S, Townsley A, Nelson GE, Moss B (2005) Poxvirus multiprotein entry-fusion complex. *Proc Natl Acad Sci USA* **102:** 18572–18577

Senkevich TG, Ward BM, Moss B (2004a) Vaccinia virus A28L gene encodes an essential protein component of the virion membrane with intramolecular disulfide bonds formed by the viral cytoplasmic redox pathway. *J Virol* **78:** 2348–2356

Senkevich TG, Ward BM, Moss B (2004b) Vaccinia virus entry into cells is dependent on a virion surface protein encoded by the A28L gene. *J Virol* **78:** 2357–2366

Slot JW, Geuze HJ (2007) Cryosectioning and immunolabeling. *Nat Protoc* **2:** 2480–2491

Smith GL, Murphy BJ, Law M (2003) Vaccinia virus motility. *Annu Rev Microbiol* **57:** 323–342

Smith GL, Vanderplasschen A, Law M (2002) The formation and function of extracellular enveloped vaccinia virus. *J Gen Virol* **83:** 2915–2931

Soltoff SP (2001) Rottlerin is a mitochondrial uncoupler that decreases cellular ATP levels and indirectly blocks protein kinase Cdelta tyrosine phosphorylation. *J Biol Chem* **276:** 37986–37992

Tillman DM, Izeradjene K, Szucs KS, Douglas L, Houghton JA (2003) Rottlerin sensitizes colon carcinoma cells to tumor necrosis factor-related apoptosis-inducing ligand-induced apoptosis via uncoupling of the mitochondria independent of protein kinase C. *Cancer Res* **63:** 5118–5125

Tokuyasu KT (1973) A technique for ultracryotomy of cell suspensions and tissues. *J Cell Biol* **57:** 551–565

Townsley AC, Moss B (2007) Two distinct low-pH steps promote entry of vaccinia virus. *J Virol* **81:** 8613–8620

Townsley AC, Weisberg AS, Wagenaar TR, Moss B (2006) Vaccinia virus entry into cells via a low-pH-dependent endosomal pathway. *J Virol* **80:** 8899–8908

Ulaeto D, Grosenbach D, Hruby DE (1996) The vaccinia virus 4c and A-type inclusion proteins are specific markers for the intracellular mature virus particle. *J Virol* **70:** 3372–3377

Vanderplasschen A, Hollinshead M, Smith GL (1998a) Intracellular and extracellular vaccinia virions enter cells by different mechanisms. *J Gen Virol* **79**(Part 4)**:** 877–887

Vanderplasschen A, Mathew E, Hollinshead M, Sim RB, Smith GL (1998b) Extracellular enveloped vaccinia virus is resistant to complement because of incorporation of host complement control proteins into its envelope. *Proc Natl Acad Sci USA* **95:** 7544–7549

Vanderplasschen A, Smith GL (1997) A novel virus binding assay using confocal microscopy: demonstration that the intracellular and extracellular vaccinia virions bind to different cellular receptors. *J Virol* **71:** 4032–4041

Wolffe EJ, Katz E, Weisberg A, Moss B (1997) The A34R glycoprotein gene is required for induction of specialized actin-containing microvilli and efficient cell-to-cell transmission of vaccinia virus. *J Virol* **71:** 3904–3915

Wolffe EJ, Vijaya S, Moss B (1995) A myristylated membrane protein encoded by the vaccinia virus L1R open reading frame is the target of potent neutralizing monoclonal antibodies. *Virology* **211:** 53–63

Zwartouw HT (1964) The chemical composition of vaccinia virus. *J Gen Microbiol* **34:** 115–123